

Effective ferromagnetic coupling between a superconductor and a ferromagnet in LaCaMnO/Nb hybrids

D. Stamopoulos,* N. Moutis, M. Pissas, and D. Niarchos

Institute of Materials Science, NCSR "Demokritos," 153-10, Aghia Paraskevi, Athens, Greece

(Received 30 September 2005; revised manuscript received 10 November 2005; published 29 December 2005)

In this work we present magnetization data on hybrids consisting of multilayers (MLs) of manganites $[\text{La}_{0.33}\text{Ca}_{0.67}\text{MnO}_3/\text{La}_{0.60}\text{Ca}_{0.40}\text{MnO}_3]_{15}$ in contact with a low- T_c Nb superconductor (SC). Although a pure SC should behave *diamagnetically* in respect to the external magnetic field in our ML-SC hybrids we observed that the magnetization of the SC follows that of the ML. Our intriguing experimental results show that the SC below its T_c^{SC} becomes *ferromagnetically* coupled to the ML. As a result in the regime where diamagnetic behavior of the SC was expected its bulk magnetization switches only whenever the coercive field of the ML is exceeded. By employing specific experiments where the ML was selectively biased or not we demonstrate that the ML inflicts its magnetic properties on the whole hybrid. Possible explanations are discussed in connection to recent theoretical proposals and experimental findings that were obtained in relative hybrids.

DOI: [10.1103/PhysRevB.72.212514](https://doi.org/10.1103/PhysRevB.72.212514)

PACS number(s): 74.78.Fk, 74.25.Ha, 85.25.Am

In recent years hybrids comprised of superconducting (SC) and ferromagnetic (FM) ingredients have attracted much interest due to the fascinating properties that they exhibit depending on the choice of materials, their specific structure, etc. Among others, basic structures of such artificial hybrids are bilayers (BLs), trilayers (TLs), and even multilayers (MLs) of homogeneous films but also distinct ferromagnetic nanoparticles (FNs) placed on top of or embedded in a SC layer.¹⁻⁶ For the case of ordered arrays of FNs it has been shown that the magnetoresistance of the SC presents distinct periodic minima at specific values of the applied magnetic field.¹⁻³ When the FNs are randomly distributed in the SC, periodic minima are not observed in the magnetoresistance but a clear enhancement in the surface-superconductivity critical field occurs when their saturation field is exceeded.^{5,6} Referring to homogeneous layered hybrids recently spin-valve devices comprised of FM-SC-FM TLs are studied intensively.⁷⁻⁹ In Refs. 7 and 9 the studied TLs employed Nb and CuNi as the SC and FM constituents, while in Ref. 8 it was studied high- T_c SC $\text{YBa}_2\text{Cu}_3\text{O}_7$ in contact with FM $\text{La}_{0.7}\text{Ca}_{0.3}\text{MnO}_3$. While in TLs comprised of low- T_c Nb (Refs. 7 and 9) the superconducting transition was increased (decreased) when the FM layers were antiparallel (parallel), in the TLs consisting of high- T_c $\text{YBa}_2\text{Cu}_3\text{O}_7$ (Ref. 8) the opposite behavior was observed.

The present work offers experimental results on hybrids consisting of MLs of manganites in direct contact with a layer of low- T_c Nb SC. We chose MLs of manganites for the constructed hybrids since we wanted to examine how the mechanism of exchange biasing^{10,11} could influence the SC. In addition, the layered structure of the ML offers enhanced coercivity which is of practical importance for the design of functional apparatus. In all samples a relatively thick FM buffer layer has been used since we expected that this should act as a main reservoir for generating stray fields that, in addition to the exchange biasing mechanism, could influence the SC. The specific manganites used for the ML are the insulating antiferromagnetic (AF) $\text{La}_{0.33}\text{Ca}_{0.67}\text{MnO}_3$ and the metallic FM $\text{La}_{0.60}\text{Ca}_{0.40}\text{MnO}_3$. Thus, each hybrid consists of a FM buffer layer followed by a ML including 15 bilayers

$[\text{La}_{0.33}\text{Ca}_{0.67}\text{MnO}_3/\text{La}_{0.60}\text{Ca}_{0.40}\text{MnO}_3]_{15}$ with a Nb layer placed on top (FM-ML-SC: which for simplicity is noticed as ML-SC). The thicknesses used are $d_{fm}=50\text{ nm}$ — $[d_{af}=4\text{ nm}/d_{fm}=4\text{ nm}]_{15}$ — $d_{sc}=100\text{ nm}$. The structure is schematically presented in Fig. 1. Two categories of ML-SC hybrids have been studied. The first category has the insulating AF $\text{La}_{0.33}\text{Ca}_{0.67}\text{MnO}_3$ as the top layer (noted as FM/AF-Nb), while the second one has the metallic FM $\text{La}_{0.60}\text{Ca}_{0.40}\text{MnO}_3$ adjacent to the Nb layer (noted as AF/FM-Nb). The same qualitative results were observed in both categories of ML-SC hybrids. Simple FM-SC bilayers have also been studied. These samples do not exhibit the effects observed in the ML-SC structures. The MLs exhibit critical temperature $T_c^{ML}=230\text{ K}$ and were prepared by pulsed laser deposition on LaAlO_3 (001) substrates.¹¹ The dc-sputtered Nb films^{5,6} have $T_c^{SC}=8.2\text{ K}$ for the ML-SC samples and $T_c^{SC}=7\text{ K}$ for the simple FM-SC bilayers. A commercial superconducting quantum interference device (SQUID) (Quantum Design) was employed for the magnetization measurements.

Our interesting magnetization data show that in the ML-SC hybrid when the SC is cooled through its T_c^{SC} under

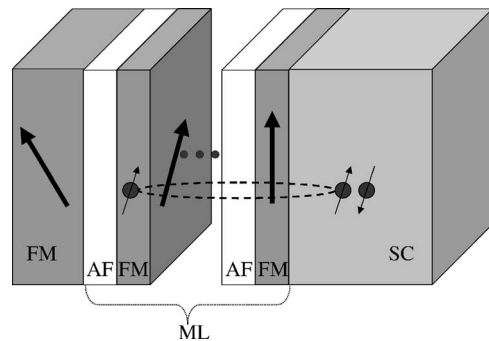


FIG. 1. Schematic representation of the ML-SC hybrid structure studied in this work. Effective ferromagnetic or antiferromagnetic coupling related to spin-triplet (parallel spins of the electrons) or spin-singlet (antiparallel spins of the electrons) superconductivity are also shown (see the discussion in the text for details). Thick arrows refer to the magnetization of each FM layer.

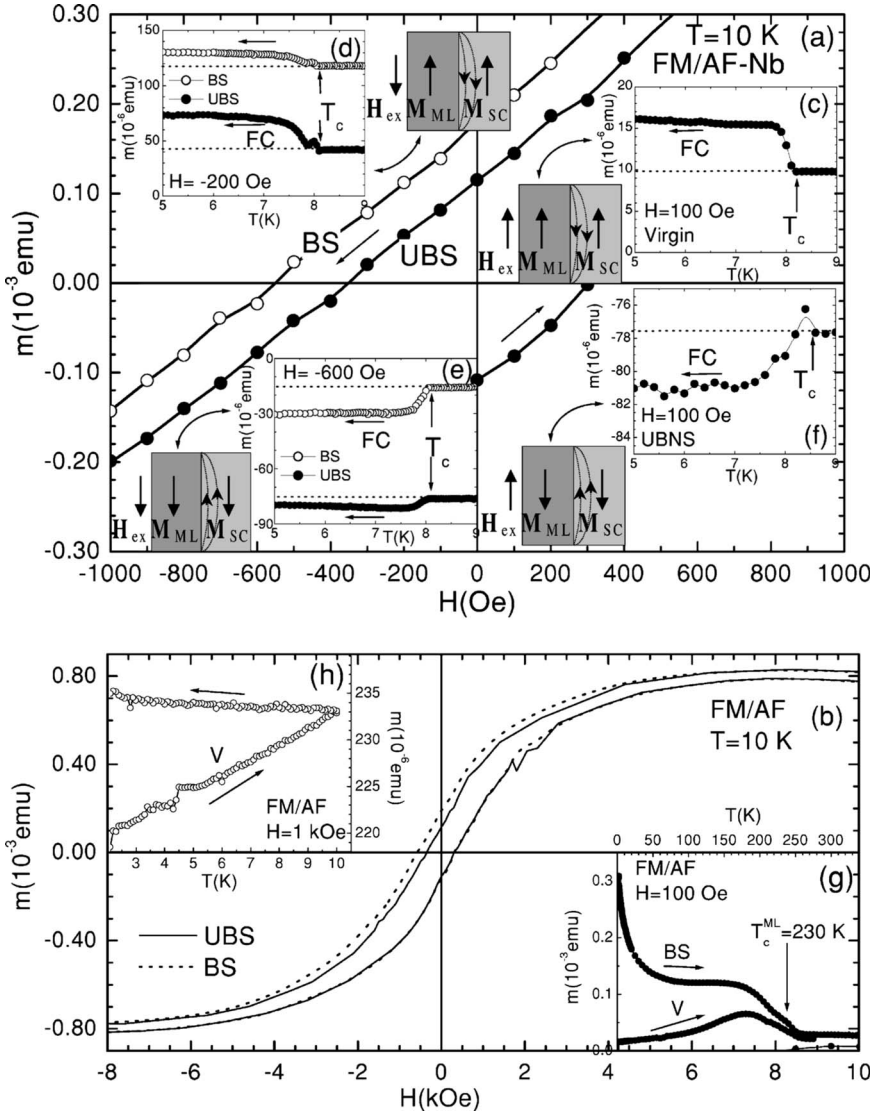


FIG. 2. Detailed magnetization data obtained in a FM/AF-Nb hybrid. In the upper panel (a) we focus on the low-field regime of the UBS and BS $m(H)$ branches obtained at $T=10$ K. The lower panel (b) shows the respective data in an extended field range. Insets (c)–(f) show $m(T)$ measurements: (c) for virgin (V) ML at $H=100$ Oe, (d) for UBS and BS ML at $H=-200$ Oe, (e) for UBS and BS ML at $H=-600$ Oe, and (f) for $H=100$ Oe when the external field is reversed once again. The relative configurations obtained for $T < T_c^{SC} = 8.2$ K of the MLs and SCs magnetizations in respect to the external magnetic field H_{ex} are shown in all cases. Curved lines denote the stray fields of the ML that penetrate the SC. Insets (g) and (h) show data for the pure ML prior to the deposition of Nb. Inset (g) show the $m(T)$ BS and V curves obtained at $H=100$ Oe for $5 \text{ K} < T < 340$ K, while inset (h) presents a detailed $m(T)$ curve obtained in the low-temperature regime for $H=1$ kOe.

the presence of a parallel magnetic field behaves as a *ferromagnet*. This is feasible since the SC layer is ferromagnetically coupled to the ML and as a consequence it has become insensitive to a reversal of the external magnetic field until the coercive field of the ML is exceeded. *When the MLs coercive field is exceeded the SCs magnetization also reverses since it follows the magnetization of the ML (switching effect)*. By performing experiments where the ML was selectively biased or not we present evidence that the ML structure separating the FM buffer and the SC layers imposes its magnetic properties on the whole hybrid. Thus, the exchange biasing mechanism could be used for regulating the magnetic field's value where the switching of the SCs magnetization occurs. The simple FM-SC bilayers studied in our work do not exhibit these features. Thus, the ML structure is an important ingredient for the generic observation of the switching effect. Possible interpretations of the obtained results are discussed.

Figures 2(a)–2(h) introduces the main results of the present work obtained in a FM/AF-Nb sample when the external magnetic field H_{ex} was parallel to its surface. In the upper panel (a) shown are the low-field parts of the $m(H)$

branches where the measurements have been performed for unbiased (UBS) and biased (BS) conditions of the ML. In the UBS (BS) the hybrid was cooled from above $T_c^{ML} = 230$ K down to $T=10$ K in zero external field, $H=0$ Oe ($H=50$ kOe). At $T=10 > T_c^{SC} = 8.2$ K the desired magnetic field was set and the magnetization was recorded while lowering the temperature until the transition of the SC was accomplished. Thus, in all measurements the SC was field cooled (FC). Insets (c)–(f) present detailed isofield $m(T)$ measurements for different magnetic histories of the ML. The lower panel (b) presents data for the pure ML prior to the deposition of the SC. In the main panel we show the BS and UBS $m(H)$ loops in an extended field regime. Inset (g) shows the respective $m(T)$ data for the ML from $T=5$ K up to room temperature. These data reveal that the mechanism of exchange bias is present in our ML. Inset (h) shows a representative detailed $m(T)$ curve in the low-temperature regime obtained at $H=1$ kOe. Such detailed data obtained in the pure ML are very important since after the deposition of the SC we should be able to distinguish the origin of any observed anomaly. We stress that we chose the FC protocol for all the performed $m(T)$ measurements for the following main

reason: in this procedure the ML shows an almost constant magnetization [see inset (h)]. Thus any detected feature in the $m(T)$ curves could safely be ascribed to the magnetic behavior of the SC.

Let us start the discussion with inset (c). These data refer to virgin ML and were obtained for positive orientation of the external field $H=100$ Oe. We see that the SCs magnetization presents a clear *increase* below its T_c^{SC} despite the fact that according to basic knowledge a *decrease* should be observed due to the diamagnetic behavior that the SC should exhibit in respect to the external field. At first sight this behavior resembles the paramagnetic effect that is usually observed in single Nb films and composite samples when FC through their critical temperature.^{12–14} As we show below the effects discussed in this work are completely different. The respective measurements for negative orientation of the external magnetic field are presented in insets (d) and (e) for both BS and UBS initial conditions of the ML. The difference between these sets of data is that in inset (d) where $H=-200$ Oe the magnetization of the ML is still positive, while in inset (e) where $H=-600$ Oe the coercive field has been exceeded so that the magnetization of the ML has changed direction. In inset (d) we clearly see again that below T_c^{SC} the magnetization of the SC presents an *increase*, while in inset (e) we see that below T_c^{SC} its magnetization *decreases*. Finally, inset (f) presents the $m(T)$ curve obtained when the external field is reversed again to positive orientation $H=100$ Oe. Since the applied field is below the coercive field of the ML we observe that the SC still exhibits a decrease below its T_c^{SC} . When the external field exceeds the coercive field of the ML the SC reverses its magnetization exhibiting an *increase* below its T_c^{SC} .

Detailed $m(T)$ data revealing the reversal of the SCs magnetization near the coercive field of the ML are presented in Figs. 3(a)–3(d) for an AF/FM-Nb sample. Panels (a) and (c) show the increasing and decreasing $m(H)$ branches, respectively, constructed from the $m(T=10$ K) data, while panels (b) and (d) show the respective $m(T)$ curves. In the data presented in panels (a)–(b) the sample was initially UBS and was set to negative saturation (the UBNS acronym in Fig. 3(b) refers to initial negative saturation). Then the field was lowered to the desired value and the $m(T)$ curve was recorded while lowering the temperature. These data clearly reveal that the SCs magnetization follows that of the ML. Despite the fact that the external field is positive the SC exhibits a negative step below its T_c^{SC} as long as the MLs magnetization is also negative, i.e., below its coercive field. When the MLs coercive field is exceeded the SC also reverses its magnetization following the ML. The data presented in (c)–(d) show a direct comparison for UBS and BS conditions for the ML. These results reveal that when the ML is BS, owing to the enhancement of its coercivity, the switching of the SCs magnetization occurs at a higher magnetic field, $H=-450$ Oe when compared with the UBS state where $H=-350$ Oe. These results propose that exchange biasing could be used as an efficient control parameter for regulating the magnetic field's value where the SC switches.

All these purely experimental data point to the situation which is presented by the respective schemes of Figs. 2(a)

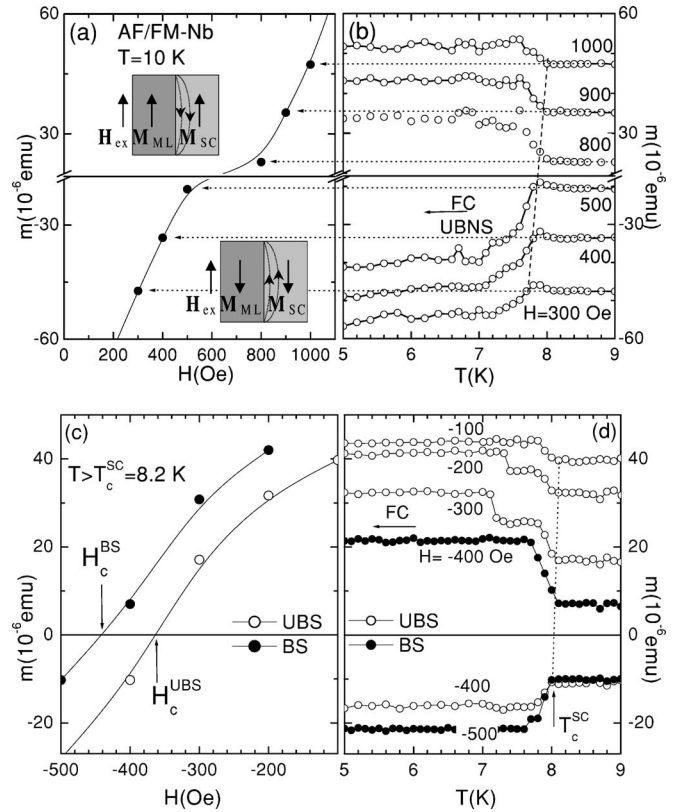


FIG. 3. Detailed data obtained in an AF/FM-Nb hybrid for various magnetic fields in the regime of the MLs coercive field. Panel (a) shows the increasing $m(H)$ branch while panel (b) shows the respective $m(T)$ curves. The relative configurations of the MLs and SCs magnetizations in respect to the external magnetic field H_{ex} are shown in both cases. Panels (c) and (d) present the respective data for UBS and BS initial conditions.

and 3(a). We see that in all cases the magnetization of the SC is aligned parallel to the one of the ML as if the Nb layer is simply an extra layer coupled ferromagnetically to the rest FM layers through the adjacent AF ones. *Macroscopically, the interpretation of the obtained results seems to relate to the stray fields that the SC experiences.* The total stray fields of both the FM buffer's and the MLs in each case are illustrated in the schemes adjacent to insets (c)–(f) of Fig. 2(a) by the curved lines. Phenomenologically, it seems that the SC is forced to behave diamagnetically not in respect to the external field but in respect to the stray fields. *Microscopically, our results may be related to recent theoretical works on the formation of spin-triplet superconductivity in FM-SC hybrids when inhomogeneous magnetization is offered to the SC by the FM.*^{15,16} In our ML-SC structures inhomogeneous magnetization is experienced by the SC owing to the specific modulated structure of the ML. The *ferromagnetic* coupling observed in our data could be ascribed to the existence of a spin-triplet component by employing an analogy of a model that originally was proposed by theory in order that the *antiferromagnetic* coupling between a SC and a FM be explained.¹⁷ According to this model since the two electrons forming a Cooper pair are well spatially separated (especially close to T_c^{SC}) the first of them may be hosted by the SC, while the second by one of the available FM layers.¹⁷ Un-

doubtedly, the spin of the second electron should be aligned ferromagnetically due to its interaction with the magnetization of the host FM layer. As a consequence the spin susceptibility of the first electron that resides in the SC could exhibit *ferromagnetic* behavior (as it is observed in our results) only in case where the two electrons of the pair have *parallel* spins, i.e., in case of triplet superconductivity. In the opposite case where spin-singlet superconductivity prevails the spin of the first electron should be *antiparallel* to the one that is hosted in the FM. As a result the SC should exhibit *antiferromagnetic* coupling to the FM. The proposed scenario is presented qualitatively in Fig. 1. The antiferromagnetic behavior was observed very recently by Stahn *et al.*¹⁸ in neutron reflectometry data obtained in $\text{La}_{2/3}\text{Ca}_{1/3}\text{MnO}_3/\text{YBa}_2\text{Cu}_3\text{O}_7$ multilayers. Their data indirectly suggested that possibly in those samples a magnetic moment was created within the SC layers that was antiparallel to the one of the FM layers as a consequence of the conventional spin-singlet electron pairing.¹⁸ In our $\text{La}_{0.60}\text{Ca}_{0.40}\text{MnO}_3$ - $[\text{La}_{0.33}\text{Ca}_{0.67}\text{MnO}_3/\text{La}_{0.60}\text{Ca}_{0.40}\text{MnO}_3]_{15}$ -Nb hybrids by means of direct magnetization measurements we observed a clear ferromagnetic coupling which, analogically, could be compatible with the formation of a spin-triplet superconducting component.¹⁵⁻¹⁷

As already discussed in the ML-SC structures studied in our work a relatively thick $\text{La}_{0.60}\text{Ca}_{0.40}\text{MnO}_3$ FM layer was used as a buffer since we expected that this should act as the main reservoir for generating stray fields that could possibly influence the SC. In addition, as a spacer between the FM buffer and the SC top layers a ML was used since we wanted to incorporate the exchange biasing mechanism. These complex ML structures are needed in order that the ferromagnetic coupling between the SC and the FM be observed. We note that the effect is *not* present in simple FM-SC bilayers constructed of $\text{La}_{0.60}\text{Ca}_{0.40}\text{MnO}_3$ and Nb ($d_{fm}=80\text{ nm}-d_{sc}=100\text{ nm}$). Representative data are shown in Figs. 4(a) and 4(b) near the coercive field of the FM where the switching of the SCs magnetization should be observed. We clearly see that the FM-SC bilayer do not exhibit the switching effect (ferromagnetic coupling) but a conventional diamagnetic behavior in respect to the external magnetic field (which notice that in this set of data is negative).

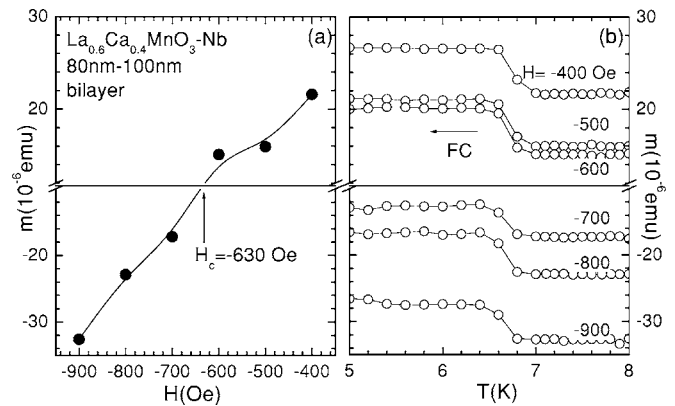


FIG. 4. (a) Decreasing branch of the $m(H)$ curve and (b) detailed FC $m(T)$ data obtained near the coercive field of the FM for a simple FM-SC bilayer. The switching of the SC is not observed in such bilayers.

Concluding, we presented experimental results in hybrids consisting of manganite MLs in contact with a Nb layer. In these samples a thick FM layer has been used as a buffer. Our results show that when the SC is FC it is ferromagnetically coupled to the ML. The SCs magnetization is not actually affected when we reverse the external magnetic field and only switches together with the magnetization of the ML when its coercive field is exceeded. The exchange biasing mechanism offered by the ML affects the behavior of the whole hybrid; the magnetic field's value where the switching of the SC occurs may be regulated by selectively biasing the ML or not. Macroscopically, our findings may be explained by suggesting that the stray fields of both the FM buffer's and the MLs may efficiently modulate the effective magnetic field experienced by the SC. Microscopically, our results may be explained by assuming the formation of spin-triplet superconductivity. The ML structure is needed for the occurrence of the discussed effects since simple FM-SC bilayers do not exhibit the same behavior. In addition to their importance to basic physics our results are promising for the design of devices based on magnetic switching processes.

*Author to whom correspondence should be addressed. Electronic address: densta@ims.demokritos.gr

¹O. Geoffroy *et al.*, J. Magn. Magn. Mater. **121**, 223 (1993); Y. Otani *et al.*, *ibid.* **126**, 622 (1993).

²D. J. Morgan and J. B. Ketterson, Phys. Rev. Lett. **80**, 3614 (1998).

³J. I. Martin *et al.*, Phys. Rev. Lett. **83**, 1022 (1999).

⁴M. Lange *et al.*, Phys. Rev. Lett. **90**, 197006 (2003).

⁵D. Stamopoulos *et al.*, Supercond. Sci. Technol. **17**, L51 (2004); D. Stamopoulos and E. Manios, *ibid.* **18**, 538 (2005).

⁶D. Stamopoulos, M. Pissas, and E. Manios, Phys. Rev. B **71**, 014522 (2005); D. Stamopoulos *et al.*, *ibid.* **70**, 054512 (2004).

⁷J. Y. Gu *et al.*, Phys. Rev. Lett. **89**, 267001 (2002).

⁸V. Pena *et al.*, Phys. Rev. Lett. **94**, 057002 (2005).

⁹A. Potenza and C. H. Marrows, Phys. Rev. B **71**, 180503(R)

(2005).

¹⁰J. Nogues and I. K. Schuller, J. Magn. Magn. Mater. **192**, 203 (1999).

¹¹N. Moutis *et al.*, Phys. Rev. B **64**, 094429 (2001).

¹²D. J. Thompson *et al.*, Phys. Rev. Lett. **75**, 529 (1995).

¹³V. A. Schweigert and F. M. Peeters, Physica C **332**, 426 (2000).

¹⁴F. B. Müller-Allinger and A. C. Mota, Phys. Rev. Lett. **84**, 3161 (2000).

¹⁵A. F. Volkov, F. S. Bergeret, and K. B. Efetov, Phys. Rev. Lett. **90**, 117006 (2003).

¹⁶F. S. Bergeret, A. F. Volkov, and K. B. Efetov, Phys. Rev. Lett. **86**, 4096 (2001).

¹⁷F. S. Bergeret, A. F. Volkov, and K. B. Efetov, Phys. Rev. B **69**, 174504 (2004).

¹⁸J. Stahn *et al.*, Phys. Rev. B **71**, 140509(R) (2005).